Hindawi
Advances in Civil Engineering
Volume 2024, Article ID 4997651, 15 pages
https://doi.org/10.1155/2024/4997651

Research Article

Cymbopogon nardus Leaf Ash as an Alternative Material for Enhancing Concrete Strength

Bunyamin Bunyamin,[1] Munirul Hady,[1] Reza Pahlevi Munirwan ,[2] and Ramadhansyah Putra Jaya [3]

[1]*Department of Civil Engineering, Faculty of Engineering, Universitas Iskandarmuda, Banda Aceh 23234, Indonesia*
[2]*Department of Civil Engineering, Faculty of Engineering, Universitas Syiah Kuala, Jln. Tgk. Syech Abdurrauf, No 7, Darussalam, Banda Aceh 23111, Indonesia*
[3]*Faculty of Civil Engineering Technology, Universiti Malaysia Pahang Al-Sultan Abdullah, Kuantan 26300, Pahang, Malaysia*

Correspondence should be addressed to Ramadhansyah Putra Jaya; ramadhansyah@ump.edu.my

Received 17 October 2023; Revised 11 December 2023; Accepted 22 December 2023; Published 19 January 2024

Academic Editor: Mahdi Salimi

Copyright © 2024 Bunyamin Bunyamin et al. This is an open access article distributed under the Creative Commons Attribution License, which permits unrestricted use, distribution, and reproduction in any medium, provided the original work is properly cited.

Numerous waste materials containing calcium and silica have been adopted as partial cement substitutes. This practice is intended to reduce the environmental impact of cement production, specifically in terms of carbon dioxide (CO_2) emissions. However, plantation waste, specifically waste from *Cymbopogon nardus* leaf, has not been completely exploited. The presence of silica in *C. nardus* leaf ash (CNLA) presents an opportunity to partially replace cement in concrete. The purpose of this study is to determine the effect of substituting CNLA at 0%, 5%, 10%, and 15% as a partial replacement for cement on the compressive and tensile strengths of concrete after 28 days of curing. For testing purposes, 15 cm × 30 cm cylindrical concrete specimens were formed. The investigation was conducted following ACI 211.1-91 (American Concrete Institute) and ASTM (American Society for Testing and Materials) standards. The required compressive strength for the concrete was 17.00 MPa. The results of the study indicate that the addition of CNLA to cement at concentrations of 0%, 5%, 10%, and 15% resulted in compressive strengths of 21.56, 21.12, 22.58, and 17.88 MPa, respectively. The results of the split tensile strength test were 2.43, 2.72, 2.87, and 3.18 MPa, respectively. According to the findings of this study, increasing the amount of CNLA in cement by 10% can increase the compressive and tensile strengths of concrete. In addition, as the percentage of CNLA exceeds 10%, the workability of the concrete decreases, posing challenges in attaining the targeted strength of the concrete.

1. Introduction

Cement is a fundamental building material used in a wide range of construction projects, including buildings, bridges, and dams [1]. Limestone accounts for 60%–65% of a typical composition of cement, and silica accounts for 17%–25% of its composition. Cement also contains alumina, iron, magnesium, sulfur, and sodium [2]. Cement production is associated with the emission of CO_2 gases, making it environmentally threatening [3–5]. Van den Heede and De Belie [6], Lee et al. [7], and Yang et al. [8] reported that the production of 1 kg of cement results in the emission of approximately 0.85 kg of carbon dioxide.

Researchers have increasingly explored the use of waste materials as eco-friendly substitutes for cement [9, 10]. Waste materials such as oyster shells [11, 12], mollusk shells [13], cockle shells [14], blood cockle shells [15], periwinkle shells [16], snail shells [17], green mussel shells [18], eggshells [19], fly ash [20], and rice husk ash [21, 22] have been extensively used as cement replacements in concrete. Utilizing waste materials as partial substitutes for cement may lower the construction production costs [23–25].

As a tropical nation, Indonesia shares a wide variety of natural resources, including an abundance of medicinal plant species. The leaves of one of these plants, *Cymbopogon nardus*, are renowned for being luxuriant and abundant. The leaves and roots of *C. nardus* are high in alkaloids, saponins, tannins, polyphenols, and flavonoids. Moreover, the foliage contains essential oils made up of various aromatic compounds [26].

C. nardus is a type of plant that produces essential oil [27, 28]. Citronella and geraniol are the primary components

Figure 1: Utilizing a temperature measurement device to burn *Cymbopogon nardus* leaves.

of *C. nardus* [29], and both have distinct fragrances [30]. The cosmetics, perfume, soap, and pharmaceutical industries typically utilize essential oils [31]. Additionally, essential oil can be used as an antifungal, antibacterial, and insect repellent [32–34]. The citronella content of *C. nardus* ranges between 0.5% and 1.5%, with the remainder consisting of solid waste (raw material residues) and distillation water [35]. Moreover, the processing of *C. nardus* into various products does not involve the disposal of its leaves, resulting in their dumping and disposal, resulting in bad smells, and environmental damage in the surrounding area [26].

When *C. nardus* leaf is burned and turned into *C. nardus* leaf ash (CNLA), it produces approximately 35.51% silica oxide, a component that is also found in cement [36]. The silica content of *C. nardus* leaf ash and rice husk ash is nearly identical [37]. Research suggests that rice husk ash can partially or completely replace cement in concrete [22, 38, 39]. The substitution of rice husk ash into cement at levels of 5%–15% can enhance the strength of concrete (compressive strength, tensile strength, and flexural strength) [21, 40].

This study investigates the effects of substituting CNLA in cement at substitution levels of 0%, 5%, 10%, and 15% by volume on concrete, as well as its effect on concrete strength (compressive and tensile strength) and workability value resulting from the incorporation of CNLA. In earlier times, *C. nardus* leaf was only utilized to produce fragrant oils; it was never incorporated into concrete. The silica content in CNLA has the potential to be used as a substitute for cement in concrete. Furthermore, this study also tries to minimize waste accumulation in the surrounding area of *C. nardus* leaves plantations, establish an optimal mix integrating CNLA, and maximize the workability, compressive strength, and tensile strength of concrete.

The CNLA utilized in this investigation originated in Aceh Tengah, Indonesia. This waste was incinerated at 500°C, sieved through a No. 200 sieve; and then substituted into cement at concentrations of 0%, 5%, 10%, and 15% using 15 cm × 30 cm cylindrical specimens. The main findings of this study include the testing of compressive and tensile strengths of concrete, which were analyzed using analysis of variance (ANOVA), and the determination of the optimal concrete strength values using Design Expert Application. In addition, XRD (X-ray diffraction), XRF (X-ray fluorescence), SEM (scanning electron microscopy), FTIR (Fourier transform infrared), and TGA–DTA (thermogravimetric analysis–differential thermal analysis) analyses were conducted to examine the different characteristics of CNLA.

2. Materials and Methods

2.1. Materials. The cement used was PCC (Portland composite cement); the fine aggregate was composed of river sand with a diameter of 4.75 mm (fine sand) and 9.50 mm (coarse sand); and the coarse aggregate has a diameter of not more than 25 mm. Fine and coarse aggregates were extracted from the Krueng Aceh River in Jantho City, Aceh Besar District, Aceh Province. The water used in this research was clean and did not contain mud or oil. The CNLA used originates from the ashes of *C. nardus* leaves burned on plantation land in Takengon, Central Aceh Regency, Aceh Province. The ashes from burning *C. nardus* leaves, which have turned into coarse particles, are collected, and then transported to the laboratory, where they are soaked in water for 24 hr to remove the dirt. Then, the ashes were heated at 105°C for 24 hr[41]. The dried coarse granules are burned manually using a combustion chamber at a temperature of 500°C, like how rice husks have been used in the past [42]. A dual-laser-equipped automatic temperature measurement instrument measures the temperature. As shown in Figure 1, the measuring instrument was positioned near the outer surface of the drum until the temperature reads 500°C. The coarse grains have a burning duration of 90 min. The CNLA was then sieved with a No. 200 sieve. The results of

(a) (b) (c)

Figure 2: The process of transforming *Cymbopogon nardus* leaves into CNLA at 500°C. (a) During burning, (b) after burning, and (c) pass sieve No. 200.

the sieve were added to the cement in the following proportions: 0%, 5%, 10%, and 15%. Figure 2 illustrates the results of converting *C. nardus* leaf waste into CNLA.

2.2. Physical Properties Analysis. The purpose of examining the physical properties of aggregate is to determine if the aggregate used in concrete mixtures satisfies the required standards. The physical properties of aggregates are examined using procedures from ASTM, including bulk density analysis (ASTM C 29/C 29M–97) [43], absorption (ASTM C 127–01) [44], specific gravity, and sieve analysis (ASTM C136–01) [45]. This investigation examines the physical properties of both fine aggregate (fine sand and coarse sand) and coarse aggregate when examining the physical properties of aggregate. Before examining the physical properties of aggregate, it was washed and sieved through sieves measuring 4.75 mm (fine sand), 9.50 mm (coarse sand), and 25 mm (coarse aggregate). The sorted fine aggregate and coarse aggregate were placed in an oven at 105°C for 24 hr to determine the bulk density of aggregate. Then, each aggregate was layered and compacted 25 times in the container. In the same way, this experiment was repeated until the third layer was filled. The aggregate-containing container was weighed, the weight was recorded, and the dimensions of container were measured. The bulk density of fine aggregate and coarse aggregate was derived from these measurements.

Similar to the previous stage, the aggregate was washed and placed in an oven at 105°C for 24 hr to determine the sieve analysis of aggregate. To verify the arrangement of coarse aggregate sieves, a sieve arrangement with the largest dimension measuring 25 mm and the smallest measuring 0.150 mm was prepared. Later, 2,000 g of coarse aggregate were placed into the sieve arrangement, filter it, and then record the weight of each sieve. The procedure for acquiring the grain arrangement for fine sand and coarse sand was identical to that for coarse aggregate. The sieve arrangement for fine sand has a maximum size of 4.75 mm and a minimum size of 0.150 mm, with 500 g of aggregate included. Meanwhile, the sieve arrangement for coarse sand with the largest size is 9.50 mm and the smallest size is 0.150 mm, with the amount of aggregate included being 1,000 g.

The aggregate was washed, sifted, and immersed in water for 24 hr to determine its specific gravity. Following that, the specific gravity of the fine aggregate was determined by observing the SSD (surface saturated dry) condition of the aggregate. For the SSD experiment, a cone-shaped container was utilized. The aggregate was layered and compacted 25 times within the cone. Then, the cone was lifted to observe the resulting decline. If the decrease is partial, the aggregate is in an SSD state, and its specific gravity can be determined using a measuring cup in the subsequent experiment. Conversely, the coarse aggregate SSD is visible visually, as the color of aggregate transforms to a white color; if the color is identical, then continue by measuring the specific gravity with a basket.

2.3. Characteristic Analysis. This investigation involved XRD, XRF, SEM, FTIR, and TGA–DTA testing to determine the characteristics of CNLA. The tests being performed seek to determine the mineral composition and structure of CNLA. XRD testing is used to analyze the composition of compounds in materials and to characterize crystals [46]. It can also be used to determine the categories of elements and compounds present in materials. This examination is conducted by inserting the sample into the XRD instrument. Then, attach the instrument to the computer and set the angle to 2θ to generate a graph of the sample's chemical compound composition. XRF testing is one of the tests used by the researchers to analyze the qualitative and quantitative chemical elements present in a substance. The sample is inserted into an XRF device and connected to a computer for this examination. Next, the computer program is run and automatically analyzed, resulting in a detailed percentage of the sample's chemical element content.

The SEM is a type of electron microscope that can produce high-resolution images of a sample's surface. Due to the

Table 1: Design specimen.

Type of concrete	Substitution of CNLA into cement (compressive strength)		Substitution of CNLA into cement (tensile strength)		Specimen name	Total specimen
	Amount of cement (%)	Amount of CNLA (%)	Amount of cement (%)	Amount of CNLA (%)		
NC	100	0	100	0	NC1 NC2 NC3 NC4 NC5	10
CNLA-5	95	5	95	5	CNLA-5.1 CNLA-5.2 CNLA-5.3 CNLA-5.4 CNLA-5.5	10
CNLA-10	90	10	90	10	CNLA-10.1 CNLA-10.2 CNLA-10.3 CNLA-10.4 CNLA-10.5	10
CNLA-15	85	15	85	15	CNLA-15.1 CNLA-15.2 CNLA-15.3 CNLA-15.4 CNLA-15.5	10

Note. NC, normal concrete for specimen number 1–5; CNLA-5%, 5% of *Cymbopogon nardus* leaf ash in cement for specimen number 1–5; CNLA-10%, 10% of *Cymbopogon nardus* leaf ash in cement for specimen number 1–5; CNLA-15%, 15% of *Cymbopogon nardus* Leaf Ash in cement for specimen number 1–5.

substitution of electrons for light waves, SEM images have qualitative characteristics in two dimensions and are useful for determining the surface structure of samples [47]. This SEM observation was performed by placing the sample on the SEM instrument and adjusting the instrument's magnification to 500 times. The results of magnification were observed, along with the surface topography of the sample. The FTIR measurement identifies the chemical composition of a substance [48]. This examination can detect chemicals in the form of compounds, atoms, or polymers. This test is conducted by focusing light on the sample, and the results are a graph of the functional groups of the solid material. The graph results are then analyzed to determine the sample's chemical characteristics. The TGA–DTA test is used to analyze the temperature-dependent behavior of a substance [49]. The purpose of this experiment is to determine the correlation between chemical reactions and temperature. This test is conducted by heating the sample at a specific location, temperature, and time until the sample's mass decreases. Therefore, this test will determine the sample's weight before and after heating it to a specific temperature.

2.4. Concrete Mix Design. Concrete mix design was calculated using the ACI 211.1-91 method [50] with a maximum aggregate diameter of 25.00 mm and a slump of 75–100 mm. The composition of the concrete was determined based on its mass in kilograms per cubic meter. In this study, CNLA was substituted for cement at concentrations of 0%, 5%, 10%, and 15%, with a diameter of 0.075 mm or passing sieve size 200. According to previous research, the quantity of waste substituted into cement ranged from 0% to 15% [51]. In addition, the research on *C. nardus* has never been conducted before; therefore, the concrete quality aimed for this study is the minimum structural concrete quality required by SNI (Indonesian National Standards), which is 17.0 MPa [52].

2.5. Specimen Design and Slump Test. The cylindrical specimen used in this study had dimensions of 150 by 300 mm. Twenty specimens were utilized for compressive strength testing, while the remaining twenty specimens were utilized for testing concrete fracturing tensile strength. Table 1 displays the planned specimens for this study.

Fine sand that has passed sieve No. 4 (4.75-mm diameter), coarse sand that has passed a 3/8″ sieve (9.50-mm diameter), and coarse aggregate that has passed a 1″ sieve (25.00-mm diameter) were weighed according to the concrete mix design results in units of kg/m^3. Moreover, a mixer machine with an 80-liter capacity was used to prepare the concrete. Accordingly, casting was carried out for every five specimens for each variation in the percentage of CNLA. Furthermore, eight times as many castings were conducted. All concrete mixing ingredients, including water, cement, coarse aggregate, coarse sand, and fine sand, are sequentially added to the mixer and stirred until the mixture was thoroughly blended. Due to the use of external materials, specifically CNLA, not all of water was used. This was done to ensure that the slump value

corresponds to what was anticipated. Therefore, at the beginning of the casting procedure, the water content was maintained between 3% and 5%, which will later be used to adjust the slump value to the target level. If, after mixing and testing for the slump, it was determined that the slump value has not decreased, the remaining water was added again. However, if the decline value decreases as expected, the remaining water does not need to be used again. The concrete mixture was then poured into the specimen mold following ASTM specifications. After 1 day, the mold was removed from the specimen, and it was immersed in an immersion chamber for 28 days. The slump test was conducted by pouring a concrete mixture into a cone-shaped container, which was then compacted 25 times in three layers. Then, the decrease that occurs upon lifting was observed and determine its scale. Next, the scale of the decline was determined to be consistent with expectations. If not, water must be added or subtracted, as explained previously.

2.6. Bulk Density Experiment. Bulk density testing was conducted in two stages: the first stage consists of compressive strength testing, and the second stage consists of tensile strength testing. Before testing compressive strength and tensile strength, the bulk density was measured, which includes four variations: bulk density for normal concrete, bulk density for 5% substitute concrete, bulk density for 10% substitute concrete, and bulk density for 15% substitute concrete. Accordingly, the bulk density test was conducted when the test object is 28-day old. After 28 days of soaking, cylindrical test objects were removed from the soaking chamber and left to dry for 12 hr. The test object was weighed three times, and its horizontal (diameter) and vertical (height) dimensions were measured. After calculating the average value, the diameter and height of the cylinder were determined. The volume of the cylinder was determined by its diameter and height. The concrete bulk density was determined by comparing the test object's mass to its volume, in kg/m^3. Using the design expert application, bulk density data were analyzed with ANOVA. ANOVA will provide a p-value that indicates whether the substitution of CNLA in cement is statistically significant. If the p-value is less than 0.05, CNLA contributes significantly to the volume weight of concrete. If $p > 0.05$, then the substitution of CNLA for cement has no significant effect on the bulk density of concrete. In addition, a graph was generated between the bulk density of concrete, the substitution percentage of CNLA, and its slump value.

2.7. Compressive Strength Experiment. The testing of compressive strength was conducted under ASTM C39/C39M-03 [53]. The specimen for the compressive strength test was a cylinder with a 150-mm diameter and a 300-mm height. The specimen was evaluated for its compressive strength when it was 28-day old. Specimens that had been submerged for 28 days were removed and allowed to dry for 12 hr in the chamber. Before testing the strength, the specimen was weighed; and its dimensions were measured to determine the bulk density of the concrete. Furthermore, the specimen's compressive strength was evaluated. The specimen was positioned in the direction of the load and placed on the testing machine. The engine was started, and the load was gradually increased. On the reading dial, it was evident that two dials were simultaneously ascending, followed by another dial descending. When one of the dials was lowered, the reading for the utmost load was recorded. Next, the concrete's compressive strength was determined through the incorporation of data. In concrete bulk density testing, data on compressive strength were analyzed with ANOVA through the design expert application, as was the case with data on compressive strength.

2.8. Split Tensile Strength Experiment. The split tensile strength of concrete was determined according to ASTM C496/496M-11 [54]. The specimen was the same as that used for compressive strength testing: a cylinder with a 150-mm diameter and 300-mm height. Testing the tensile strength of concrete uses the same procedure as testing the compressive strength of the concrete. The primary distinction was in the orientation of loading, where the specimen was positioned parallel to the load. The machine was turned on, with the load being increased steadily until it reaches its maximum capacity, testing the compressive strength of concrete. Afterward, data processing were performed to derive the concrete's split tensile strength. As with the compressive strength test, the results of the concrete tensile strength test were analyzed using ANOVA within the design expert application.

3. Results and Discussion

3.1. Results of Aggregate Physical Properties Test. Examination of the aggregate's physical properties includes fine aggregate (fine sand and coarse sand) and coarse aggregate. The examination of the aggregate's physical properties was conducted in the laboratory, and the results are presented in Table 2.

According to Table 2, the bulk density of fine sand, coarse sand, and coarse aggregate are 1,697, 1,848, and 1,736 kg/l, respectively. Previous researchers have suggested that a suitable bulk density of aggregate is greater than 1,400 kg/l [55]. The value obtained was still within the specified limits. The specific gravities of fine sand, coarse sand, and coarse aggregate were 2.755, 2.744, and 2.834, respectively. According to a previous research by Orchard et al. [56], an acceptable aggregate's specific gravity should be greater than 2.600. The specific gravity value obtained was consistent with this finding. The obtained total absorption value was 2% lower. According to the previous research, a reasonable absorption value for aggregates occurs between 0% and 2% [55]. The FM values obtained for fine sand, coarse sand, and coarse aggregate were 2.34, 2.92, and 6.83, respectively. According to the previous research, a suitable FM for fine sand is between 1.50 and 3.80, for coarse sand between 2.90 and 3.20, and coarse aggregate between 5.5 and 8.0 [57]. The results of analyzing the aggregate's physical properties indicate that the aggregate in this investigation can be used as material in the production of concrete.

3.2. Characteristic Test Result. The purpose of XRD examination is to determine the crystal structure, phase, degree of

Table 2: Physical properties of aggregate result.

No.	Material	Bulk density (kg/l)	Specific gravity	Absorption (%)	Fineness modulus (FM)
1.	Fine sand	1697	2.755	1.613	2.34
2.	Coarse sand	1848	2.744	1.632	2.92
3.	Coarse aggregate	1736	2.834	1.929	6.83

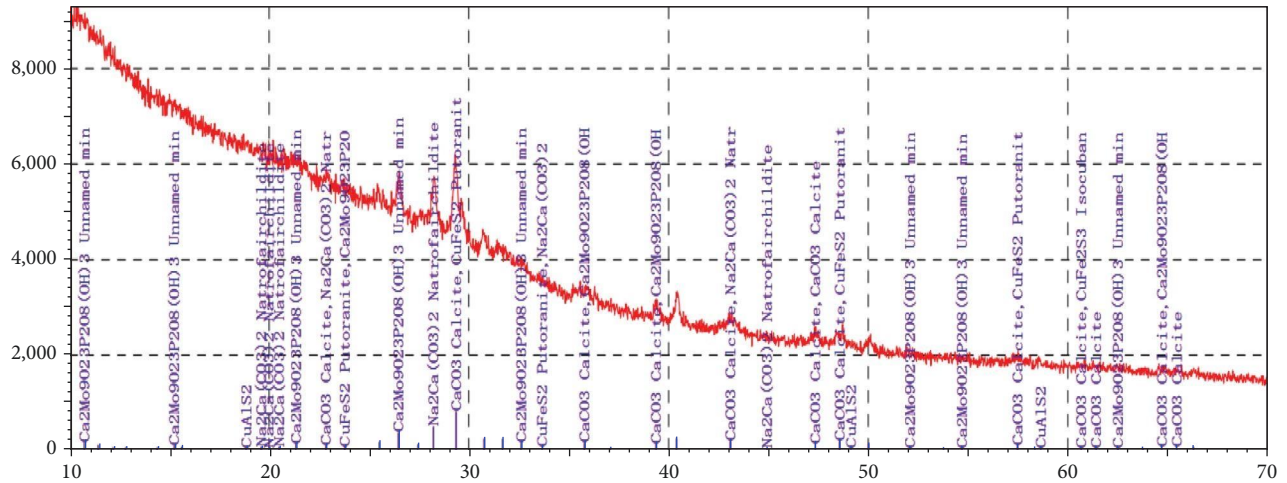

Figure 3: XRD test results for CNLA burned at 500°C.

crystallinity, lattice parameters, and the types of elements and compounds present in a material. Figure 3 displays the results of XRD measurements on CNLA.

Based on the XRD test results (Figure 3), several compounds were identified in CNLA burned at 500°C, namely: $CaCO_3$, $CUFeS_2$, $Ca_2Mo_9O_{23}P_2O_8(OH)_3$, $CuAlS_2$, $Na_2Ca(CO_3)_2$, and $CuFe_2S_3$. The graph demonstrates that CNLA has a dominant phase of calcite ($CaCO_3$) crystal structure. The calcite crystal structure was formed at the following angles (2θ): 23°, 29°, 36°, 39°, 43°, 47°, 48°, 57°, 61°, and 65°. The highest calcium carbonate diffraction peak was observed at (2θ) = 23°, according to Figure 3. This calcium carbonate diffraction yields marginally different results than previous studies. The highest calcium carbonate diffraction peak was observed at (2θ) = 29.5°, according to Han et al. [58].

The purpose of XRF analysis was to determine the chemical elements present in a solid or liquid sample. Based on XRF testing, the chemical element analysis of CNLA obtained the results presented in Table 3. According to Table 3, approximately 32% of CNLA was composed of the element Si, or silica. In addition, around 11% of CNLA was composed of calcium. The two predominant components of CNLA share characteristics with cement. According to the previous researchers, the primary components of cement are silica and calcium [59].

SEM examination was utilized to examine the material's microscopic structure and surface. Figure 4 shows the SEM test results of CNLA incinerated at 500°C, which have been magnified 1,000 times, 2,000 times, and 3,000 times. The morphological characteristics of the CNLA sample are evident from Figure 4(a): It consists of rectangular particles displaying a rough surface. The particles exhibit a range of lengths, with an average diameter of 10 μm. Certain particles contain very fine gaps. The particle spacing is nearby, with only minor voids present in a fraction of the particles.

Table 3: XRF test results of CNLA (with mass of 225 mg/cm^2) burned at 500°C.

No.	Component	Mass (%)
1	MgO	0.704
2	Al_2O_3	0.537
3	SiO_2	32.0
4	P_2O_5	2.01
5	SO_3	1.16
6	Cl	1.08
7	K_2O	11.5
8	CaO	11.0
9	MnO	0.839
10	Fe_2O_3	1.34
11	CuO	0.0186
12	ZnO	0.129
13	Br	0.0204
14	Rb_2O	0.0527
15	SrO	0.0720
16	Dy_2O_3	0.0471
17	Balance	37.5

According to the data presented in Figure 4(b), CNLA displays a morphological characteristic of long, irregular particles measuring an average of 10 μm in diameter with open-edge separations. The surface is uneven in texture and

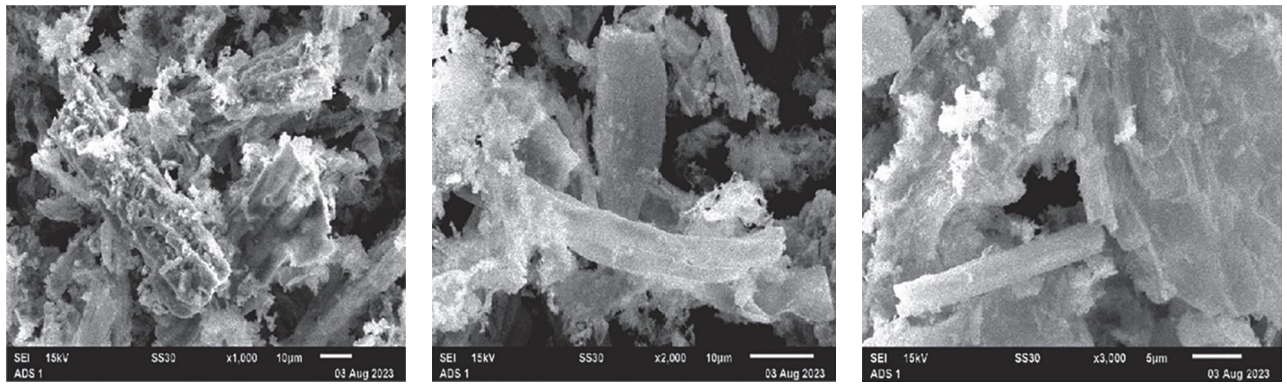

(a) (b) (c)

Figure 4: SEM test results for CNLA burned at 500°C. (a) 1,000 times magnification, (b) 2,000 times magnification, and (c) 3,000 times magnification.

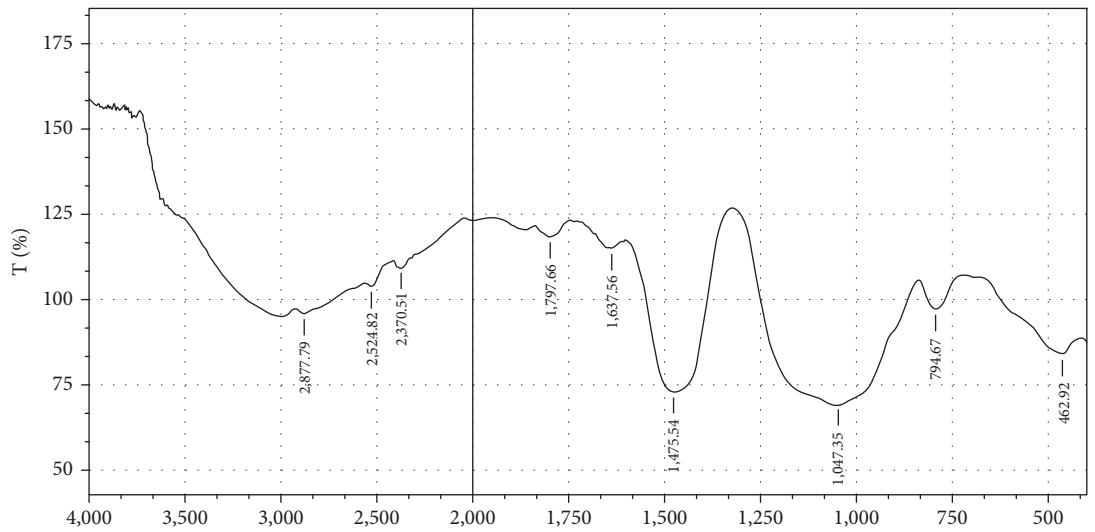

Figure 5: FTIR test results for CNLA burned at 500°C.

partially smooth. There are major gaps between the particles, and their separation is not particularly close.

The morphological characteristics of CNLA are evident in Figure 4(c), which depicts the presence of thin sheets and lengthy particles featuring smooth surfaces. The mean size at a magnification of 3,000 times is 5 μm. Compacted masses are observed at the top of the sheet. The only area where a minor gap forms is in the center.

Functional groups in solid and liquid samples can be determined using FTIR analysis. Figure 5 depicts the results of the FTIR examination. On the basis of this image, it was evident that CNLA incinerated at 500°C forms several compound bonds, namely C—H, O—H, and C—H. C—H functional group was formed at an absorption of 2,877.79 cm^{-1} with alkane compounds; the O—H functional group was formed at an absorption of 2,524.82 cm^{-1} with alcohol and phenol (H bond) compounds; and the C—H functional group was formed at an absorption of 794.67 cm^{-1} with alkene compounds. CaO was detected in the highest absorption band, namely 2,877.79 cm^{-1}, which corresponds to the C—H functional group peak (Figure 5). The FTIR measurement results were consistent with the previous research [60].

The TGA–DTA test was conducted to determine the sample's weight loss and heat emission after being heated to a specific temperature. Figure 6 displays the TGA–DTA test results for CNLA. The TGA curve in Figure 6(a) indicates that the weight of CNLA decreases by 14.45% during heating from room temperature to 600°C. The loss of weight in CNLA was the result of water evaporation. Moreover, Figure 6(b) depicts a DTA curve with a heat discharge of −596.91 cal/g.

3.3. Concrete-Mix Design Results. The concrete arrangement was planned according to the ACI rules, which were based on weight in kg/m^3 units. Table 4 displays the concrete-mixture design results. The proposed compressive strength of the concrete in this study was 17.00 MPa. Based on the planned compressive strength, the ACI Table provides a w/c (water cement ratio) of 0.62. Table 4 indicates that the bulk density of concrete is 2,380 kg/m^3. According to previous research,

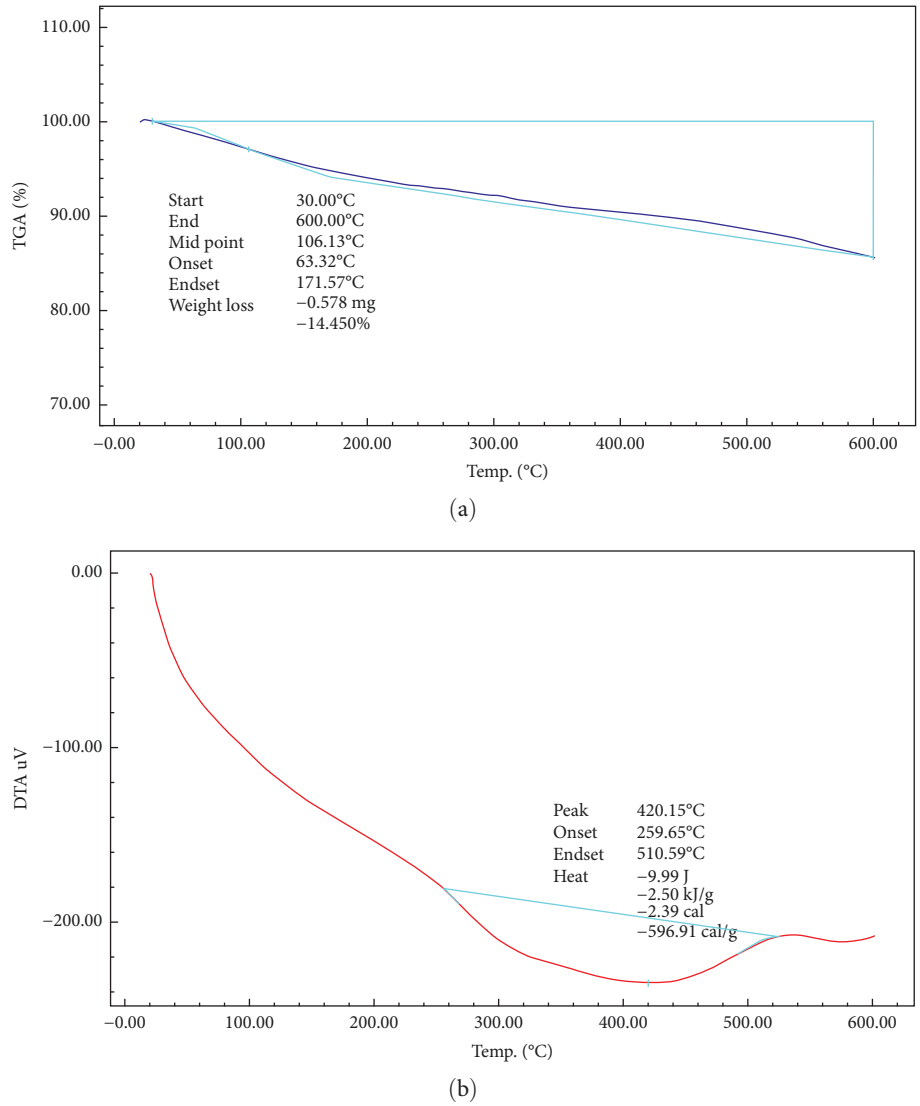

Figure 6: DTA–TGA test of CNLA burned at 500°C. (a) TGA test of CNLA burned at 500°C. (b) DTA test of CNLA burned at 500°C.

Table 4: Results of concrete mix design with w/c of 0.62.

No.	Material	Amount (kg/m^3)
1.	Water	193.00
2.	Cement	310.70
3.	Coarse aggregate	119.16
4.	Coarse sand	307.98
5.	Fine sand	370.16
Total		2,380.00

the bulk density of concrete produced for a design compressive strength of 17.0 MPa is 2,380 kg/m^3 [61]. In addition, the obtained bulk density of concrete value is close to the average bulk density of concrete value, which is 2,400 kg/m^3 [62].

3.4. Slump Test Result. The intended slump in this study was 75–100 mm, following ACI regulations. Using a concrete mixing machine, five specimens were mixed for each mixture of concrete-forming materials. Thus, eight trials of the collapse test were conducted, with each trial containing five specimens. Each experiment provides a slump value or reduction in the concrete mixture. The decline value was examined to determine whether it was decreased as anticipated. Adding or subtracting water was necessary if tests do not meet the plan. For more details, it can be seen in Table 5.

According to Table 5, the slump values obtained for the compressive strength and tensile strength specimens follow the same pattern: the greater the quantity of CNLA substituted in the cement, the harder the concrete mixture was to mix. Other studies by Attah et al. [63–66] have come to similar conclusions. To achieve the planned slump, the quantities of cement and water must be increased, as shown in Table 5. The addition of cement and water was essential because the slump test did not decrease, necessitating multiple trials to achieve the desired slump of 75–100 mm. The addition of cement and water (workability) in this study was because excessive absorption occurs and $Ca(OH)_2$ was

Table 5: Slump test result.

Type of concrete	Specimen for compressive strength testing		Specimen for tensile strength testing	
	Height of slump value (mm)	Workability (±w/c)	Height of slump value (mm)	Workability (±w/c)
NC	76.00	−3%	82.00	−3%
CNLA-5	80.00	+3%	86.00	+3%
CNLA-10	82.00	+7%	84.00	+7%
CNLA-15	92.00	+11%	88.00	+11%

Table 6: Experimental design for bulk density and compressive strength testing.

Run	Factor 1 A:CNLA substitution (%)	Factor 2 B:Slump value (mm)	Response 1 Bulk density (kg/m^3)	Response 2 Compressive strength (MPa)
1	0	76	2,462.09	21.56
2	5	80	2,460.41	21.12
3	10	82	2,459.41	22.58
4	15	92	2,455.51	17.88

Table 7: Model summary statistics and ANOVA for bulk density response.

Source	Sum of squares	df	Mean square	F-value	p-Value	
Model	23.38	2	11.69	25,256.00	0.0044	Significant
A-CNLA substitution	0.0303	1	0.0303	65.54	0.0782	—
B-Slump value	1.87	1	1.87	4,045.43	0.0100	—
Residual	0.0005	1	0.0005	—	—	—
Cor total	23.38	3	—	—	—	—

Table 8: Analysis of compressive strength test results using ANOVA.

Source	Sum of squares	df	Mean square	F-value	p-Value	
Model	12.34	2	6.17	208.36	0.0489	Significant
A-CNLA substitution	3.85	1	3.85	129.82	0.0557	—
B-Slump value	7.76	1	7.76	261.81	0.0393	—
Residual	0.0296	1	0.0296	—	—	—
Cor total	12.37	3	—	—	—	—

produced more rapidly when these materials are combined with cement [67].

3.5. Test Results for Bulk Density and Compressive Strength of Concrete. The analysis of the test results for the bulk density and compressive strength of concrete was conducted using ANOVA. The parameters considered in the analysis were variations in the substitution of CNLA in cement and the slump value. Table 6 displays the design parameters and corresponding responses utilized in the analysis of test data related to the bulk density and compressive strength of concrete. The results for evaluating the bulk density and compressive strength of concrete were analyzed through the design expert application using ANOVA based on the design parameters and responses shown in Table 6.

Table 7 shows the model summary statistics and the ANOVA for the bulk density response, respectively. The results of measuring the bulk density of concrete are highly significant ($p < 0.05$), as shown in the table. This indicates that substituting CNLA for cement has a significant impact on the bulk density of concrete. The F-value for the results of the statistical analysis of bulk density was found to be 25,256.00. This indicates that the obtained model is significant, with a 0.44% error rate. The Predicted R^2 of 0.9982 is in reasonable agreement with the adjusted R^2 of 0.9999; i.e., the difference is less than 0.2.

The results of the concrete compressive strength test were also analyzed using ANOVA and the design expert application. Table 8 shows the model summary statistics and the ANOVA for the compressive strength response, respectively. The results of measuring the compressive strength of concrete are significant ($p < 0.05$), as shown in the table. This indicates that the substitution of CNLA for cement has a significant impact on the increase in concrete

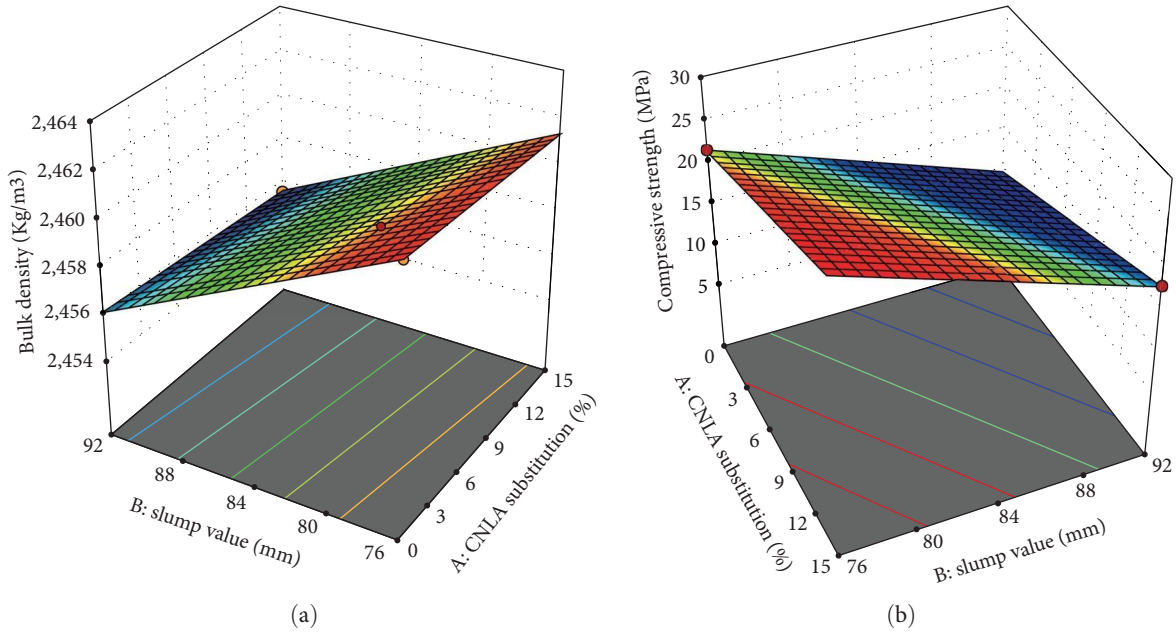

(a) (b)

Figure 7: Test results for bulk density and compressive strength of concrete. (a) Bulk density testing. (b) Compressive strength testing.

Table 9: Optimization of concrete compressive strength.

Number	CNLA substitution	Slump value	Bulk density	Compressive strength	Desirability	
1	11.099	80.930	2,459.752	23.942	1.000	Selected

compressive strength. According to the statistical analysis of compressive strength, the F-value was determined to be 208.36. This indicates that the model obtained has a significant error rate of 4.89%. The predicted R^2 of 0.7766 is not as close to the adjusted R^2 of 0.9928 as one might normally expect; i.e., the difference is more than 0.2.

Using a linear graphic model and the results of laboratory tests on the bulk density and compressive strength of concrete, a graph of the bulk density and compressive strength of concrete can be made using the parameters CNLA substitution and slump value. The results of the concrete bulk density and compressive strength experiments are shown in Figure 7. Based on Figure 7(a), the minimum bulk density of concrete is approximately 2,455.51 kg/m^3, and the maximum is approximately 2,462.09 kg/m^3. When CNLA is added to cement, the bulk density of the concrete decreases. Attah et al. stated similarly that the bulk density of concrete decreases proportionally with the amount of oyster shell ash substituted for cement [68]. Figure 7(b) shows that the minimum compressive strength of concrete is approximately 17.88 MPa and the maximum is approximately 22.58 MPa. By substituting 10% CNLA for cement, the compressive strength of concrete can be increased. This is because the cement hydration process can react with the existing CaO and SiO_2 and distributing them equitably in the correct proportions. The compressive strength of concrete decreases by 5% when CNLA is substituted. This is because the CaO in CNLA does not react effectively with the CaO in cement. A 15% substitution of CNLA resulted in a decrease in the compressive strength of the concrete. Due to the excessive SiO_2 content, the CaO content in cement can no longer react with silica (saturation occurs). The results of this study are consistent with prior research that suggested variations in the compressive strength of concrete could result from the addition of periwinkle to cement at concentrations of 0%, 5%, 10%, and 15%, with the corresponding values being 17.6, 17.0, 19.1, and 16.8 MPa [69]. Additional research findings indicate that varying percentages (0%, 4%, 6%, and 8%) of clam shell ash substituted for cement can induce variations in the compressive strength of concrete. Specifically, the following compressive strength values were obtained: 45.0, 38.6, 47.8, and 32.6 MPa [70]. This study's compressive strength test results are comparable to those found in Bai et al.'s [71] research, which found that the substitution of nano silica in cement at concentrations of 0%, 0.6%, 0.9%, and 1.2% resulted in varying compressive strengths. The compressive strength of concrete decreases when nano silica is substituted into cement by 0.6%, but increases when substituted at 0.9%, and subsequently, the compressive strength decreases when substituted by 1.2%. However, the obtained compressive strength was consistent with predictions [71].

Based on the results of testing the bulk density and compressive strength of concrete, the design expert application was optimized to achieve maximum concrete compressive strength. Based on the optimization results, 100 concrete compressive strength maximization solutions were generated. Table 9 is one of 100 solutions produced based on variations in the percentage of CNLA (0%–15%) and slump

Table 10: Experimental design for bulk density and tensile strength testing.

Run	Factor 1 A:CNLA substitution (%)	Factor 2 B:Slump value (mm)	Response 1 Bulk density (kg/m^3)	Response 2 Tensile strength (MPa)
1	0	82	2,494.30	2.43
2	5	86	2,491.14	2.72
3	10	84	2,445.01	2.87
4	15	88	2,441.84	3.18

Table 11: Analysis of bulk density test results using ANOVA.

Source	Sum of squares	df	Mean square	*F*-value	*p*-Value	
Model	2,440.01	2	1,220.01	4.880E + 07	0.0001	Significant
A-CNLA substitution	1,821.19	1	1,821.19	7.285E + 07	<0.0001	—
B-slump value	369.20	1	369.20	1.477E + 07	0.0002	—
Residual	0.0000	1	0.0000	—	—	—
Cor total	2,440.01	3	—	—	—	—

Table 12: Analysis of tensile strength test results using ANOVA.

Source	Sum of squares	df	Mean square	*F*-value	*p*-Value	
Model	0.2925	2	0.1462	1,462.50	0.0185	Significant
A-CNLA substitution	0.0720	1	0.0720	720.00	0.0237	—
B-slump value	0.0045	1	0.0045	45.00	0.0942	—
Residual	0.0001	1	0.0001	—	—	—
Cor total	0.2926	3	—	—	—	—

value (75–100 mm), with an ideal desirability value of 1.0. Based on Table 9, the maximum compressive strength of concrete is calculated to be 23.942 MPa. This indicates that the maximum compressive strength of concrete can be obtained if 11.10% CNLA is substituted for cement and the slump value is 81 mm.

3.6. Test Results for Bulk Density and Tensile Strength of Concrete. The bulk density and tensile strength experiments of concrete were analyzed using ANOVA with the following parameters: variations in CNLA substitution into cement and slump value. Table 10 displays the design parameters and responses for analyzing the bulk density and tensile strength test results for concrete.

Based on the design parameters and responses shown in Table 10, the bulk density test results were analyzed using ANOVA via the design expert application. Table 11 shows the model summary statistics and the ANOVA for the bulk density response, respectively.

The results of measuring the bulk density of concrete are statistically significant ($p < 0.05$), as shown in the table. This significant result demonstrates the same trend as the bulk density measurement in Table 7, namely that it has an important influence on the concrete bulk density. The *F*-value for the results of the statistical analysis of bulk density was 4.88×10^7. This indicates that the obtained model is accurate, with an error rate of 0.01%. The predicted R^2 of 1.0000 is in reasonable agreement with the adjusted R^2 of 1.0000; i.e., the difference is less than 0.2.

The results of the concrete tensile strength test were also analyzed using ANOVA via the design expert application. Table 12 shows the model summary statistics and the ANOVA for the tensile strength response, respectively.

The table displays that the results of measuring the tensile strength of concrete are statistically significant ($p < 0.05$). This indicates that the substitution of CNLA for cement significantly increases the tensile strength of concrete. The *F*-value for the results of the statistical analysis of tensile strength was found to be 1,462.50. This indicates that the obtained model is significant, with a 1.85% error rate. The predicted R^2 of 0.9945 is in reasonable agreement with the adjusted R^2 of 0.9990; i.e., the difference is less than 0.2.

Based on the results of laboratory testing of the bulk density and tensile strength of concrete, a graph of the bulk density and tensile strength of concrete can be created by integrating the parameters CNLA substitution and slump value with a linear graphic model, as illustrated in Figure 8. Based on Figure 8(a), the minimum bulk density of concrete is approximately 2,441.84 kg/m^3, and the maximum is approximately 2,494.30 kg/m^3. More CNLA reduces the bulk density of concrete. The results of this bulk density test follow the same pattern as the previous bulk density test. Figure 8(b) shows that the minimum tensile strength of concrete is approximately 2.43 MPa and the maximum is approximately

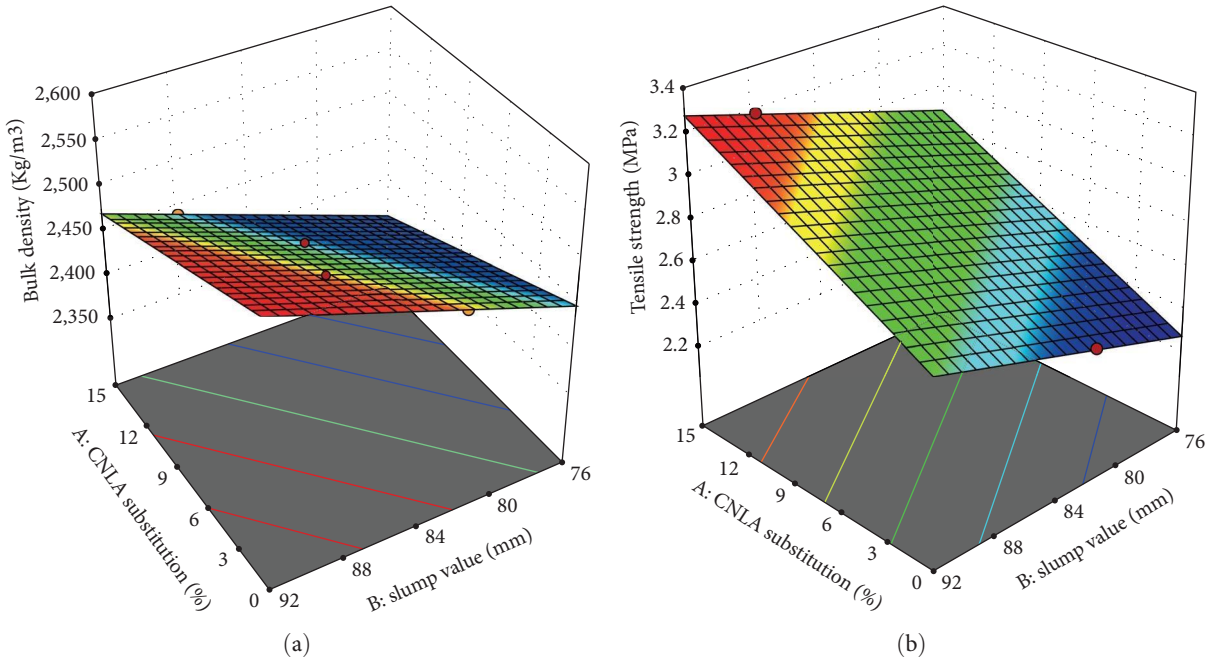

Figure 8: Test results for bulk density and tensile strength of concrete. (a) Bulk density testing. (b) Tensile strength testing.

Table 13: Optimization of concrete tensile strength.

Number	CNLA substitution	Slump value	Bulk density	Tensile strength	Desirability	
1	13.332	93.758	2,493.683	3.252	1.000	Selected

3.18 MPa. By substituting 15% CNLA for cement, the tensile strength of concrete can be increased. This is because the cement hydration process can react with the existing CaO and SiO_2 and distribute them equitably in the correct proportions. [13] stated that by converting oyster shell waste into oyster shell ash and substituting 15% of the ash into cement, the tensile strength of concrete could be significantly increased. Other researchers have also reported that substituting 5%–15% rice husk ash for cement can improve the tensile strength of concrete [21, 40]. In contrast to the trend observed in the compressive strength of concrete, which increases with a 10% CNLA substitution, the tensile strength of concrete experiences an increase at a 15% CNLA substitution. This is because the CNLA sample consists of irregularly shaped, oval, and rectangular particulates with a rough surface. CNLA has a morphological structure comparable to that of fiber. While the incorporation of fiber into concrete can generally enhance its tensile strength, it does not guarantee a substantial improvement in its compressive strength [55]. Consequently, as the tensile load increases, the CNLA morphology can start deforming. As the number of CNLA substitutions in cement increases, so does the number of fiber-like particles; consequently, the tensile strength rises.

Based on the results of testing the bulk density and tensile strength of the concrete, the design expert application was used to optimize the concrete to achieve the highest possible tensile strength. Based on the optimization results, 100 solutions were obtained to generate the maximum tensile strength of concrete. Table 13 is one of one hundred solutions generated based on variations in the percentage of CNLA (0%–15%) and slump value (75–100 mm), with an ideal desirability value of 1.0. The maximum tensile strength of concrete, according to Table 13, is 3.252 MPa. This indicates that the optimum tensile strength of concrete can be attained if CNLA is added to cement at a ratio of 13.33% and the slump value is 94 mm.

4. Conclusion

The findings of the study demonstrate that the substitution of CNLA to cement at varying concentrations of 0%, 5%, 10%, and 15% resulted in compressive strengths of 21.56, 21.12, 22.58, and 17.88 MPa. Moreover, the split tensile strength test showed findings of 2.43, 2.72, 2.87, and 3.18 MPa, respectively.

The results of the research indicate that increasing the use of CNLA in cement by 10% can increase the compressive and tensile strength of concrete. However, if CNLA is substituted over 10%, workability decreases, and it becomes difficult to achieve the target concrete strength. Furthermore, the utilization of CNLA as a replacement for cement has the potential to reduce agricultural waste, hence providing

environmental advantages. This is because CNLA is readily available and contains similar chemical components to cement, namely SiO_2 and CaO.

Data Availability

The (figure/table) data used to support the findings of this study are included within the article.

Conflicts of Interest

The authors declare that they have no conflicts of interest.

Acknowledgments

The support provided by Lembaga Layanan Pendidikan Tinggi Wilayah XIII; Direktorat Riset, Teknologi dan Pengabdian kepada Masyarakat; Kementerian Pendidikan, Kebudayaan, Riset, dan Teknologi in the form of a research grant vote number 036/LL13/AL.04/LT/2023 for this study is highly appreciated.

References

[1] UN Environment, S. K. L. Scrivener, V. M. John, and E. M. Gartner, "Eco-efficient cements: potential economically viable solutions for a low-CO_2 cement-based materials industry," *Cement and Concrete Research*, vol. 114, pp. 2–26, 2018.

[2] G. Marino and Y. D. Setiyarto, "Penggunaan tanah liat untuk mengurangi jumlah semen pada beton geopolimer," *CRANE: Civil Engineering Research Journal*, vol. 1, no. 2, 2020.

[3] M. F. Alnahhal, T. Kim, and A. Hajimohammadi, "Waste-derived activators for alkali-activated materials: a review," *Cement and Concrete Composites*, vol. 118, Article ID 103980, 2021.

[4] J. J. Biernacki, J. W. Bullard, G. Sant et al., "Cements in the 21st century: challenges, perspectives, and opportunities," *Journal of the American Ceramic Society*, vol. 100, no. 7, pp. 2746–2773, 2017.

[5] J. Di Filippo, J. Karpman, and J. R. DeShazo, "The impacts of policies to reduce CO emissions within the concrete supply chain," *Cement and Concrete Composites*, vol. 101, pp. 67–82, 2019.

[6] P. Van den Heede and N. De Belie, "Environmental impact and life cycle assessment (LCA) of traditional and 'green'-concretes: literature review and theoretical calculations," *Cement and Concrete Composites*, vol. 34, no. 4, pp. 431–442, 2012.

[7] M. Lee, W.-S. Tsai, and S.-T. Chen, "Reusing shell waste as a soil conditioner alternative? A comparative study of eggshell and oyster shell using a life cycle assessment approach," *Journal of Cleaner Production*, vol. 265, Article ID 121845, 2020.

[8] K.-H. Yang, Y.-B. Jung, M.-S. Cho, and S.-H. Tae, "Effect of supplementary cementitious materials on reduction of CO_2 emissions from concrete," *Journal of Cleaner Production*, vol. 103, pp. 774–783, 2015.

[9] Y. Izumi, A. Iizuka, and H.-J. Ho, "Calculation of greenhouse gas emissions for a carbon recycling system using mineral carbon capture and utilization technology in the cement industry," *Journal of Cleaner Production*, vol. 312, Article ID 127618, 2021.

[10] D. L. Summerbell, C. Y. Barlow, and J. M. Cullen, "Potential reduction of carbon emissions by performance improvement: a cement industry case study," *Journal of Cleaner Production*, vol. 135, pp. 1327–1339, 2016.

[11] J. H. Seo, S. M. Park, B. J. Yang, and J. G. Jang, "Calcined oyster shell powder as an expansive additive in cement mortar," *Materials*, vol. 12, no. 8, Article ID 1322, 2019.

[12] O. A. Ubachukwu and F. O. Okafor, "Investigation of the supplementary cementitious potentials of oyster shell powder for eco-friendly and low-cost concrete," *Electronic Journal of Geotechnical Engineering*, vol. 24, no. 5, pp. 1297–1306, 2019.

[13] A. P. Adewuyi, S. O. Franklin, and K. A. Ibrahim, "Utilization of mollusc shells for concrete production for sustainable environment," *International Journal of Scientific and Engineering Research*, vol. 6, 2015.

[14] N. O. R. Hazurina, A. B. B. Hisham, D. M. Mat, and M. J. M. Azmi, "Potential use of cockle (anadaragranosa) shell ash as partial cement replacement in concrete," *Caspian Journal of Applied Sciences Research*, vol. 2, pp. 369–376, 2013.

[15] M. Olivia, R. Oktaviani, and Ismeddiyanto, "Properties of concrete containing ground waste cockle and clam seashells," *Procedia Engineering*, vol. 171, pp. 658–663, 2017.

[16] U. D. Offiong and G. E. Akpan, "Assessment of physico-chemical properties of periwinkle shell ash as partial replacement for cement in concrete," *International Journal of Scientific Engineering and Science*, vol. 1, no. 7, pp. 33–36, 2017.

[17] J. R. Dankwah and E. Nkrumah, "Recycling blends of rice husk ash and snail shells as partial replacement for Portland cement in building block production," *Ghana Journal of Technology*, vol. 1, pp. 67–74, 2016.

[18] P. Lertwattanaruk, N. Makul, and C. Siripattarapravat, "Utilization of ground waste seashells in cement mortars for masonry and plastering," *Journal of Environmental Management*, vol. 111, pp. 133–141, 2012.

[19] S. Paruthi, A. H. Khan, A. Kumar et al., "Sustainable cement replacement using waste eggshells: a review on mechanical properties of eggshell concrete and strength prediction using artificial neural network," *Case Studies in Construction Materials*, vol. 18, Article ID e02160, 2023.

[20] M. A. Bahedh and M. S. Jaafar, "Ultra high-performance concrete utilizing fly ash as cement replacement under autoclaving technique," *Case Studies in Construction Materials*, vol. 9, Article ID e00202, 2018.

[21] F.-C. Lo, M.-G. Lee, and S.-L. Lo, "Effect of coal ash and rice husk ash partial replacement in ordinary Portland cement on pervious concrete," *Construction and Building Materials*, vol. 286, Article ID 122947, 2021.

[22] I. Said, B. Khan, O. Inderyas, M. A. Rahman, and S. Ahmed, "Utilization of rice husk ash as a pozzolan in self compacting concrete," *International Journal of Civil Engineering and Technology*, vol. 8, no. 1, Article ID IJCIET_08_01_011, 2017.

[23] Á. Kuki, L. Nagy, M. Zsuga, and S. Kéki, "Fast identification of phthalic acid esters in poly (vinyl chloride) samples by direct analysis in real time (DART) tandem mass spectrometry," *International Journal of Mass Spectrometry*, vol. 303, no. 2-3, pp. 225–228, 2011.

[24] R. P. Munirwan, M. R. Taha, A. Mohd Taib, and M. Munirwansyah, "Shear strength improvement of clay soil stabilized by coffee husk ash," *Applied Sciences*, vol. 12, no. 11, Article ID 5542, 2022.

[25] J. M. Paris, J. G. Roessler, C. C. Ferraro, H. D. DeFord, and T. G. Townsend, "A review of waste products utilized as supplements to Portland cement in concrete," *Journal of Cleaner Production*, vol. 121, pp. 1–18, 2016.

[26] S. A. F. Kawengian, J. Wuisan, and M. A. Leman, "Uji daya hambat ekstrak daun serai (*Cymbopogon citratus* L) terhadap pertumbuhan *Streptococcus mutans*," e-GiGi 5, 2017.

[27] N. L. Arpiwi, I. K. MUksin, and N. L. Kartini, "Essential oil from *Cymbopogon nardus* and repellant activity against Aedes aegypti," *Biodiversitas Journal of Biological Diversity*, vol. 21, no. 8, 2020.

[28] P. Vyshali, K. J. T. Saraswathi, and G. R. Mallavarapu, "Chemical composition of the essential oils of *Cymbopogon citratus* (DC.) stapf grown in three locations in south India," *Journal of Essential Oil Bearing Plants*, vol. 18, no. 1, pp. 230–235, 2015.

[29] M. Rafi, A. Kautsar, D. A. Septaningsih et al., "Feasibility of near-infrared spectroscopy and chemometrics analysis for discrimination of *Cymbopogon nardus* from *Cymbopogon citratus*," *Arabian Journal of Chemistry*, vol. 15, no. 12, Article ID 104277, 2022.

[30] U. Rastuti, "Konversi limbah penyulingan daun cengkeh dan daun sereh menjadi kompos," Prosiding 8, 2019.

[31] D. C. J. Weng, J. Latip, S. A. Hasbullah, and H. Sastrohamidjojo, "Optimal extraction and evaluation on the oil content of citronella oil extracted from *Cymbopogon nardus*," *Malaysian Journal of Analytical Science*, vol. 19, pp. 71–76, 2015.

[32] S. R. Ishkeh, M. Asghari, H. Shirzad, A. Alirezalu, and G. Ghasemi, "Lemon verbena (*Lippia citrodora*) essential oil effects on antioxidant capacity and phytochemical content of raspberry (*Rubus ulmifolius* subsp. *sanctus*)," *Scientia Horticulturae*, vol. 248, pp. 297–304, 2019.

[33] J. O. W. Gonzalez, E. N. Jesser, C. A. Yeguerman, A. A. Ferrero, and B. F. Band, "Polymer nanoparticles containing essential oils: new options for mosquito control," *Environmental Science and Pollution Research*, vol. 24, no. 20, pp. 17006–17015, 2017.

[34] C. Yeguerman, E. Jesser, M. Massiris, C. Delrieux, A. P. Murray, and J. O. W. González, "Insecticidal application of essential oils loaded polymeric nanoparticles to control German cockroach: design, characterization and lethal/sublethal effects," *Ecotoxicology and Environmental Safety*, vol. 189, Article ID 110047, 2020.

[35] R. Solekha, P. A. I. Setiyowati, B. Musyarofah, S. Nisah, M. A. Bianto, and B. D. Jauhari, "Penyulingan minyak atsiri serai wangi dengan metode stabilitas suhu dan lama penyulingan untuk meningkatkan rendemen," *Journal of Biology Education, Science & Technology*, vol. 6, no. 1, pp. 120–126, 2023.

[36] C. N. Naiborhu, "Efek Penggunaan Abu Daun Serai (Kandungan 0%–17, 5%) Sebagai Bahan Substitusi Parsial Semen Terhadap Kuat Tekan Beton," 2021.

[37] S. Sahoo, P. K. Parhi, and B. C. Panda, "Durability properties of concrete with silica fume and rice husk ash," *Cleaner Engineering and Technology*, vol. 2, Article ID 100067, 2021.

[38] S. Fernando, C. Gunasekara, D. W. Law, M. C. M. Nasvi, S. Setunge, and R. Dissanayake, "Life cycle assessment and cost analysis of fly ash—rice husk ash blended alkali-activated concrete," *Journal of Environmental Management*, vol. 295, Article ID 113140, 2021.

[39] T. Luukkonen, Z. Abdollahnejad, J. Yliniemi, P. Kinnunen, and M. Illikainen, "Comparison of alkali and silica sources in one-part alkali-activated blast furnace slag mortar," *Journal of Cleaner Production*, vol. 187, pp. 171–179, 2018.

[40] S. Sathe, M. Z. Kangda, and S. Dandin, "An experimental study on rice husk ash concrete," *Materials Today: Proceedings*, vol. 77, Part 3, pp. 724–728, 2022.

[41] S. Kaewdaeng, P. Sintuya, and R. Nirunsin, "Biodiesel production using calcium oxide from river snail shell ash as catalyst," *Energy Procedia*, vol. 138, pp. 937–942, 2017.

[42] M. Haque, S. Ray, A. F. Mita, S. Bhattacharjee, and M. J. B. Shams, "Prediction and optimization of the fresh and hardened properties of concrete containing rice husk ash and glass fiber using response surface methodology," *Case Studies in Construction Materials*, vol. 14, Article ID e00505, 2021.

[43] ASTM, "29/C 29M-97. Stand. Test Method Bulk Density," Unit Weight. Voids Aggreg, 2010.

[44] S.ASTM, "Standard test method for density, relative density (specific gravity), and absorption of coarse aggregate," C127-12, 2012.

[45] ASTMC136-01, "C136-01. Stand. Test method sieve anal," Fine Coarse Aggregates, 2003.

[46] J. Sánchez-Molina, D. Álvarez-Rozo, J. F. Gelves-D\'\iaz, and F. A. Corpas-Iglesias, "Coffee husk as substitute material for clay in the manufacturing of ceramic materials in construction in the metropolitan area of Cucuta," 2018, Recuper. https://core.ac.uk/download/pdf/230560171.pdf.

[47] P. A. S. Araújo, R. M. Andrade, A. J. M. Araújo et al., "Cordierite-based ceramics with coffee husk ash addition: I —microstructure and physical properties," *Journal of Materials Research and Technology*, vol. 15, pp. 2471–2483, 2021.

[48] W. K. Hareru, F. B. Asfaw, and T. Ghebrab, "Physical and chemical characterization of coffee husk ash effect on partial replacement of cement in concrete production," *International Journal of Sustainable Construction Engineering Technology*, vol. 13, no. 1, pp. 167–184, 2022.

[49] F. Tibola, T. de Oliveira, D. Cerqueira, C. Ataíde, and C. Cardoso, "Kinetic parameters study for the slow pyrolysis of coffee residues based on thermogravimetric analysis," *Química Nova*, vol. 43, pp. 426–434, 2020.

[50] N. Hasan and N. Hasan, "Concrete mixture design," in *Durability and Sustainability of Concrete*, pp. 37–61, Springer, Cham, 2020.

[51] B. Bunyamin, R. P. Munirwan, M. Ridha, and N. Hendrifa, "Utilization of wood processing dust as a substitute for a part of cement in concrete," *IOP Conference Series: Materials Science and Engineering*, vol. 1087, Article ID 12004, 2021.

[52] B. S. Nasional, "Persyaratan beton struktural untuk bangunan gedung dan penjelasan," (SNI 2847: 2019), 2019.

[53] A. Standard, *C39/C39M–20 Standard Test Method for Compressive Strength of Cylindrical Concrete Specimens*, ASTM, Conshohocken, PA, 2020.

[54] ASTMC496/C496M-11, "Standard test methodfor splitting tensile strength for cylindricalconcrete specimens," A.S.T.M. Int. WestConshohocken P.A vol. 04.02 p. 5., 2011.

[55] M. S. Shetty and A. K. Jain, *Concrete Technology (Theory and Practice)*, S. Chand Publishing, Ram Nagar, New Delhi, 2019.

[56] D. F. Orchard, A. Curran, and R. Hearne, "Concrete technology," in *Properties of Materials*, vol. 1, Applied Science Publishers, United Kingdom, 1979.

[57] ASTMC33-97, "C 33-97: Standard specification for concrete aggregates," Annu. B. ASTM Stand. 4, 1997.

[58] Y. Han, R. Lin, and X.-Y. Wang, "Sustainable mixtures using waste oyster shell powder and slag instead of cement: performance and multi-objective optimization design," *Construction and Building Materials*, vol. 348, Article ID 128642, 2022.

[59] K. Yamada, "Basics of analytical methods used for the investigation of interaction mechanism between cements and

superplasticizers," *Cement and Concrete Research*, vol. 41, no. 7, pp. 793–798, 2011.

[60] P. Raizada, P. Shandilya, P. Singh, and P. Thakur, "Solar light-facilitated oxytetracycline removal from the aqueous phase utilizing a H_2O_2/$ZnWO_4$/CaO catalytic system," *Journal of Taibah University for Science*, vol. 11, no. 5, pp. 689–699, 2018.

[61] B. Bunyamin, F. D. Kurniasari, R. P. Munirwan, and R. Putra Jaya, "Effect of coral aggregates of blended cement concrete subjected to different water immersion condition," *Advances in Civil Engineering*, vol. 2022, Article ID 2919167, 10 pages, 2022.

[62] N. M. Ibrahim, R. Che Amat, S. Salehuddin, N. L. Rahim, A. R. Abdul Razak, and W. H. Ooi, "Properties of lightweight concrete composites with mixture of fly ash and concrete sludge aggregate," *Technology Evolution for Silicon Nano-Electronics*, vol. 594, pp. 482–486, 2014.

[63] I. C. Attah, R. K. Etim, and D. U. Ekpo, "Behaviour of periwinkle shell ash blended cement concrete in sulphuric acid environment," *Nigerian Journal of Technology*, vol. 37, no. 2, pp. 315–321, 2018.

[64] R. K. Etim, I. C. Attah, and O. B. Bassey, "Assessment of periwinkle shell ash blended cement concrete in crude oil polluted environment," *FUW Trends in Science & Technology Journal*, vol. 2, no. 2, pp. 879–885, 2017.

[65] Y. Liao, X. Wang, L. Wang, Z. Yin, B. Da, and D. Chen, "Effect of waste oyster shell powder content on properties of cement–metakaolin mortar," *Case Studies in Construction Materials*, vol. 16, Article ID e01088, 2022.

[66] K. O. Olusola and A. A. Umoh, "Strength characteristics of periwinkle shell ash blended cement concrete," *International Journal of Architecture, Engineering and Construction*, vol. 1, pp. 213–220, 2012.

[67] B. Da, H. Yu, H. Ma, Y. Tan, R. Mi, and X. Dou, "Experimental investigation of whole stress–strain curves of coral concrete," *Construction and Building Materials*, vol. 122, pp. 81–89, 2016.

[68] I. C. Attah, R. K. Etim, and J. E. Sani, "Response of oyster shell ash blended cement concrete in sulphuric acid environment," *Civil and Environmental Research*, vol. 11, no. 4, pp. 62–74, 2019.

[69] B. R. Etuk, I. F. Etuk, and L. O. Asuquo, "Feasibility of using sea shells ash as admixtures for concrete," *Journal of Environmental Science and Engineering A*, vol. 1, pp. 121–127, 2012.

[70] B. P. Ong and U. Kassim, "Performance of concrete incorporating of clam shell as partially replacement of ordinary Portland cement (OPC)," *Journal of Advance Research in Applied Mechanics*, vol. 55, no. 1, pp. 12–21, 2019.

[71] S. Bai, X. Guan, H. Li, and J. Ou, "Effect of the specific surface area of nano-silica particle on the properties of cement paste," *Powder Technology*, vol. 392, pp. 680–689, 2021.